

Communication

Not peer-reviewed version

Microwave-Assisted Hydrothermal Synthesis of Hydroxyapatite Flakes as Substrates for Titanium Dioxide Film Deposition

[Néstor Méndez-Lozano](#)*, Eduardo E. Perez-Ramirez, Miguel de la Luz-Asunción

Posted Date: 8 March 2024

doi: 10.20944/preprints202403.0482.v1

Keywords: Hydroxyapatite; Titanium dioxide films; Hydroxyapatite flakes; Substrate deposition; Morphological characterization.



Preprints.org is a free multidiscipline platform providing preprint service that is dedicated to making early versions of research outputs permanently available and citable. Preprints posted at Preprints.org appear in Web of Science, Crossref, Google Scholar, Scilit, Europe PMC.

Copyright: This is an open access article distributed under the Creative Commons Attribution License which permits unrestricted use, distribution, and reproduction in any medium, provided the original work is properly cited.

Disclaimer/Publisher's Note: The statements, opinions, and data contained in all publications are solely those of the individual author(s) and contributor(s) and not of MDPI and/or the editor(s). MDPI and/or the editor(s) disclaim responsibility for any injury to people or property resulting from any ideas, methods, instructions, or products referred to in the content.

Communication

Microwave-Assisted Hydrothermal Synthesis of Hydroxyapatite Flakes as Substrates for Titanium Dioxide Film Deposition

Néstor Méndez-Lozano ^{*}, Eduardo E. Pérez-Ramírez and Miguel de la Luz-Asunción

Universidad del Valle de México, Campus Querétaro, Blvd. Juriquilla no. 1000 A Del. Santa Rosa Jáuregui, C.P. 76230, Querétaro, Qro., México.; nestor.mendez@uvmnet.edu; eduardo_perezr@my.uvm.edu.mx; miguel_delaluz@my.uvm.edu.mx

^{*} Correspondence: nestor.mendez@uvmnet.edu (N.M.-L.)

Abstract: This article describes the synthesis of hydroxyapatite (HAp) flakes through a microwave-assisted hydrothermal method. These flakes are intended for use as substrates for depositing titanium dioxide (TiO_2) films using chemical vapor deposition with metal-organic precursors (MOCVD). The results reveal the formation of crystalline hydroxyapatite characterized by a uniform morphology. Additionally, we demonstrated the successful deposition of TiO_2 coatings on the hydroxyapatite flakes, resulting in a distinctive faceted prism morphology. Our findings affirm the effective synthesis of the HAp/ TiO_2 composite material. To further explore the material's practical applications, we recommend assessing the photocatalytic activity of these composite membranes in future research.

Keywords: hydroxyapatite; titanium dioxide films; hydroxyapatite flakes; substrate deposition; morphological characterization

1. Introduction

In recent years, the global escalating environmental challenges have intensified the exploration of using TiO_2 photocatalysts as a promising solution. These materials have predominantly found application in the remediation of pollutants in both water and air due to their versatility [1]. While powdered catalysts have demonstrated efficacy, they are not without limitations, particularly concerning challenges in stirring and subsequent separation processes [2]. In contrast, thin-film catalysts have emerged as a viable alternative, overcoming these drawbacks with multiple potential applications.

Various studies have investigated the preparation of thin TiO_2 coatings utilizing diverse synthesis techniques such as spray-coating, sol-gel, and chemical vapor deposition (CVD) [3–5]. The inherent advantage of thin TiO_2 coatings lies in their seamless integration onto substrates with irregular shapes and expansive surface areas. Recent studies have underscored the pivotal role played by morphology and crystalline structure in influencing the photocatalytic activity of these coatings [6,7].

Despite the substantial progress in this field, there remains a noteworthy gap in the literature regarding the utilization of hydroxyapatite as a substrate for TiO_2 thin films. While studies have explored various substrates such as quartz, glass, silicon, and aluminum [8], the potential of hydroxyapatite has not been extensively investigated. Previous research examined hydroxyapatite as a photocatalyst in the aqueous phase [9], albeit limited by its high band-gap energy, restricting its use to UV irradiation.

In a noteworthy departure from conventional studies, recent investigations have demonstrated the exceptional photocatalytic oxidation activity of hydroxyapatite–titanium (HAp/ TiO_2) composite materials [10]. The innovation lies in harnessing the remarkable co-absorbent properties of

hydroxyapatite, resulting in a substantial enhancement in photocatalytic activity. Furthermore, the environmentally friendly nature of hydroxyapatite as a calcium compound adds an extra dimension to its appeal. HAp/TiO₂ composites offer unique advantages for TiO₂ coatings, particularly in biomedical and photocatalytic applications where enhanced biocompatibility and performance are desired. While they may involve higher initial costs and more complex fabrication processes than pure titanium substrates, the benefits they provide justify their use in specific applications where their properties are advantageous.

In the current study, we present a novel approach synthesizing TiO₂ thin films on hydroxyapatite (HAp) substrates. Our methodology involves microwave-assisted synthesis to produce hydroxyapatite flakes and chemical vapor deposition using metal-organic precursors to achieve the desired coatings. This multifaceted synthesis strategy aims to capitalize on the unique properties of hydroxyapatite and TiO₂, offering a potential breakthrough in the development of advanced photocatalytic materials with enhanced efficiency and environmental sustainability. The goal of this study is to comprehensively analyze the morphological and structural properties of this hydroxyapatite-titanium (HAp/Ti) composite material. Specifically, we aim to investigate crystalline hydroxyapatite flakes as an efficient substrate for titanium dioxide coatings. Furthermore, we suggest innovative uses for the HAp/Ti composite material, thereby contributing to the development of future research in this field.

2. Materials and Methods

Materials: Calcium nitrate [Ca(NO₃)₂], glutamic acid [C₅H₉NO₄], potassium phosphate [K₂HPO₄], and potassium hydroxide [KOH]. Distilled water was used in all synthesis steps.

Calcium nitrate [Ca(NO₃)₂] (1.16 g) and glutamic acid [C₅H₉NO₄] (4.35 g) were mixed in 300 ml of distilled water, to which glutamic acid was slowly added. The solution was stirred for 55 min at 70 °C. Meanwhile, potassium phosphate [K₂HPO₄] (1.12 g) and potassium hydroxide [KOH] (0.76 g) were mixed in 100 ml of distilled water. The solution was stirred for 15 min at 85 °C. Then, both solutions were mixed dropwise and stirred for 20 min at 85 °C. Finally, 20 glasses with 20 ml of solution were placed in the microwave oven (Monowave). The microwave conditions were a 200 °C temperature, a 10 min heating ramp, a 45 min reaction time, and a 55 min cooling time [11].

Once the process in the microwave oven was completed, the solid phase was filtered and washed with deionized water. The samples were placed in a desiccator at room temperature to obtain the hydroxyapatite flakes (HAp). The next step was to deposit the TiO₂ thin films on the HAp flakes using the metal-organic chemical vapor deposition technique (MOCVD) [12]. For this, 10 ml of acetone mixed with 20 ml of titanium isopropoxide was used as a precursor. The synthesis parameters are shown in Table 1, and the schematic diagram of the synthesis process is shown in Figure 1.

Table 1. TiO₂ deposition conditions using pulsed injection.

Substrate Temperature (°C)	Injectors Pressure (psi)	Argon Flow (l/min)	Injection Frequency (ms)
500	4.5	0.11	250

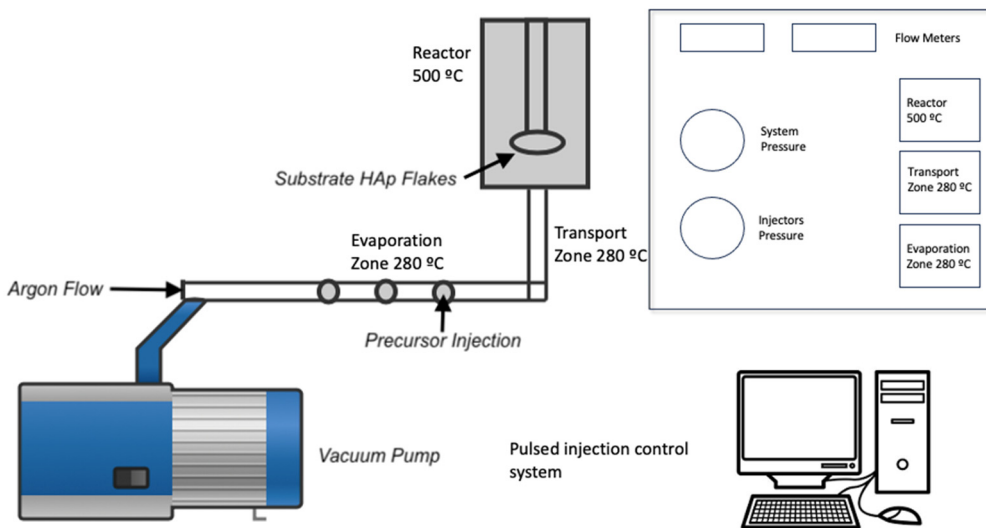


Figure 1. Schematic diagram to obtain TiO_2 coatings on hydroxyapatite flakes.

2.1. Phase Composition: X-ray Diffraction (XRD)

X-ray powder diffraction was used to identify the crystalline phases contained in all the samples. Wide-angle X-ray experiments were carried out using a Rigaku Mini Flex diffractometer and $\text{Cu } \mathbf{k}_{\alpha}$ radiation ($\lambda = 1.5406 \text{ \AA}$), an accelerating voltage of 40 kV, and a current of 30 mA. Diffractograms were recorded with a Solid-State D/teX-ULTRA Detector from 5 to 80° on a 2θ scale and a rate of 10° per minute. The spectrum analysis software MDI Jade V 5.0.37 was used [11].

2.2. Morphology and Microstructure: Scanning Electron Microscopy (SEM)

Morphological, topological, and microstructural analyses of all the samples were carried out using a JEOL JXA-8530F Scanning Electron Microscope. The analysis was performed using a 20 kV electron acceleration voltage, and the secondary electrons formed the images. All the samples were placed on a stainless-steel plate with a separation of 5 mm, pasted with silver paint, and covered with a gold thin film through sputtering to avoid the electrostatic charge accumulation [11].

2.3. Elemental Composition: Dispersive-Energy Spectroscopy (EDS)

To obtain the elemental composition of HAp/ TiO_2 powders, an Electronic Microprobe for Microanalysis (EPMA) JXA - 8530F was used. The operation conditions were a voltage of 10 kV and a current of 0.10 nA. A small tablet was made from each sample, and then each tablet was coated with a graphite thin film [11].

3. Results and Discussion

We present diffractograms and micrographs of both sides of the flakes (Figure 2). XRD (X-Ray diffraction) studies show the crystal structure corresponding to hydroxyapatite according to the Powder Diffraction File (PDF) # 01-084-1998 (Figure 2a). The observed Bragg reflections indicate a preferential direction of growth in the (100) plane due to the use of glutamic acid during the synthesis process [12]. On the other hand (Figure 2b), the diffraction pattern corresponding to the TiO_2 coating is shown, where the indexed reflections correspond to the anatase phase of TiO_2 and the pattern shows low-intensity and well-defined peaks; however, background noise is observed. Additionally, SEM (scanning electron microscopy) micrographs of uncoated HAp flakes (Figure 2c) and TiO_2 -coated HAp flakes are shown (Figure 2d). The HAp side shows a morphology of agglomerated plaques. This morphology is characteristic of the hydroxyapatite plaques reported in previous studies [13]. The TiO_2 coating (Figure 1d) shows a uniform film free of cracks, where the formation of

nanostructures with well-defined faces is observed, indicating step-by-step growth. This growth occurs due to the MOCVD synthesis process using a metal-organic precursor [14].

The flakes show a compact structure; however, they can easily be divided into hydroxyapatite rods. As is well-established, the crystalline structure of hydroxyapatite is formed through the assembly of Ca type I (trigonal prisms), Ca type II (pentagonal dipyramids), phosphate groups (tetrahedra), and OH groups. The interaction mechanism of glutamic acid with this structure enables the incorporation with type I calcium, thereby inhibiting growth in the c-direction of the structure. This inhibition promotes growth in the a and b directions, consequently resulting in a plate-like morphology.

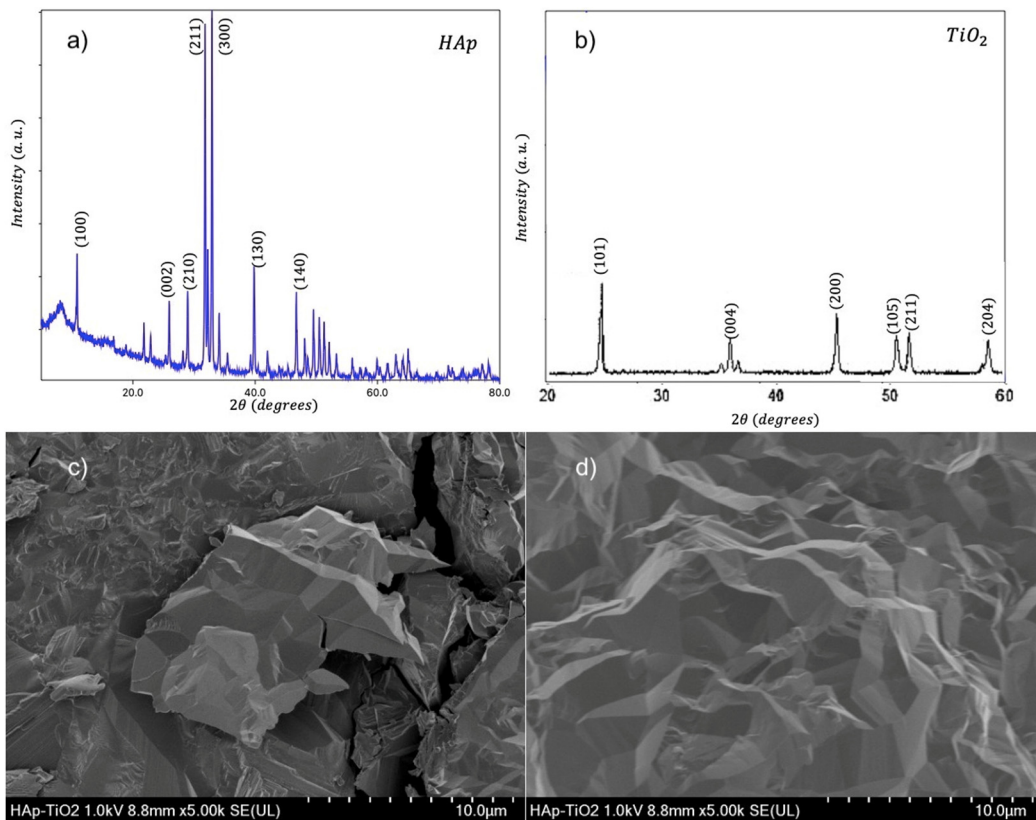


Figure 2. a) XRD diffraction pattern of HAp flake; b) XRD diffraction pattern of TiO₂-coated flake; c) SEM micrograph of HAp; d) SEM micrograph of TiO₂.

Micrographs of the hydroxyapatite flakes and TiO₂ thin films are shown (Figure 3). The hydroxyapatite flakes show a homogeneous morphology with some reliefs at magnifications of 5000x (Figure 3a); in addition, agglomerated plates with dimensions of 10 μm can be observed (Figure 3b) at 2000x.

Likewise, the observed plates are composed of agglomerated rods. This morphology is characteristic of the hydroxyapatite obtained through hydrothermal methods [15]. Hydroxyapatite flakes are obtained depending on the amount of glutamic acid used in the synthesis process and the filtering of the sample when leaving the microwave oven. Micrographs of the TiO₂ thin film at 5000x magnification (Figure 3c) and 2000x magnification (Figure 3d) are also shown. Both micrographs show the typical morphology of TiO₂ films obtained through MOCVD [16]. The MOCVD process allows a coating on the upper face of the hydroxyapatite flake, and a structure of densely packed crystals with a faceted prism appearance are observed. At the lowest magnification, the crystals can be observed forming a flower-like morphology. This might be due to the rearrangement of the deposited crystals. After the initial deposition of the crystals, the rearrangement process begins with their nucleation. This involves the formation of small groups of crystals from the initial material, causing flower-like growth.

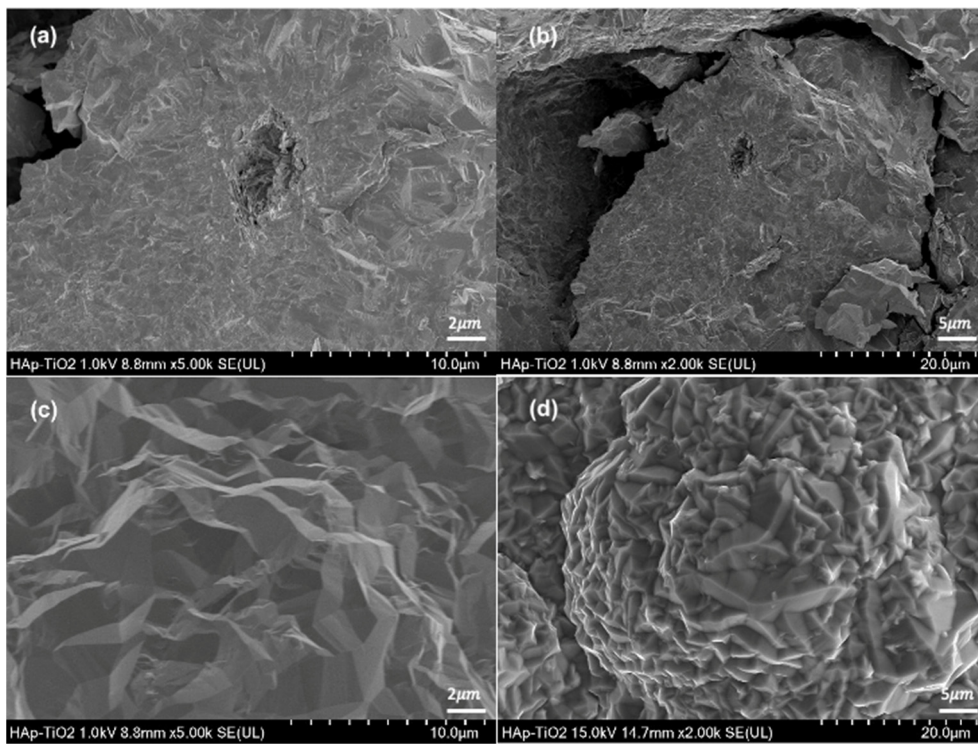


Figure 3. a) SEM micrograph of HAp flakes at 5000x; b) SEM micrograph of HAp flakes at 2000x; c) SEM micrograph of TiO₂ at 5000x; d) SEM micrograph of TiO₂ to 2000x.

EDS (energy-dispersive spectroscopy) elemental composition analyses were performed on the TiO₂ thin films (Figure 4). The results shown at 500x (Figure 4a) and 5000x (Figure 4b) magnifications reveal that the peaks predominantly correspond to Ti (titanium) and O (oxygen) and that the presence of aluminum in the spectra is due to the sample holder used during the analysis. High, sharp peaks indicate that the thin films are of high purity and were successfully deposited on the substrate. The presence of Ca and P is not visible in the spectra because only the TiO₂-coated part was analyzed. The atomic percentage of Ti in the sample was 30.89 % on average. The EDS results agree with the previous DRX and SEM studies, demonstrating that the elemental composition of the thin films allowed us to determine the chemical composition of the samples. Numerous studies have considered this method for composition analysis [17]. In the EDS study, the accelerating voltage of the electron beam had a significant influence on the obtained results [18]. In Figure 5, the EDS spectrum for the hydroxyapatite flakes is depicted, revealing the presence of calcium and phosphorus with a Ca/P ratio of 1.69. Additionally, both spectra exhibit a trace amount of aluminum, measured at 0.56 wt.%. This aluminum presence is likely attributed to contamination from impurities in the gases utilized during the MOCVD synthesis process.

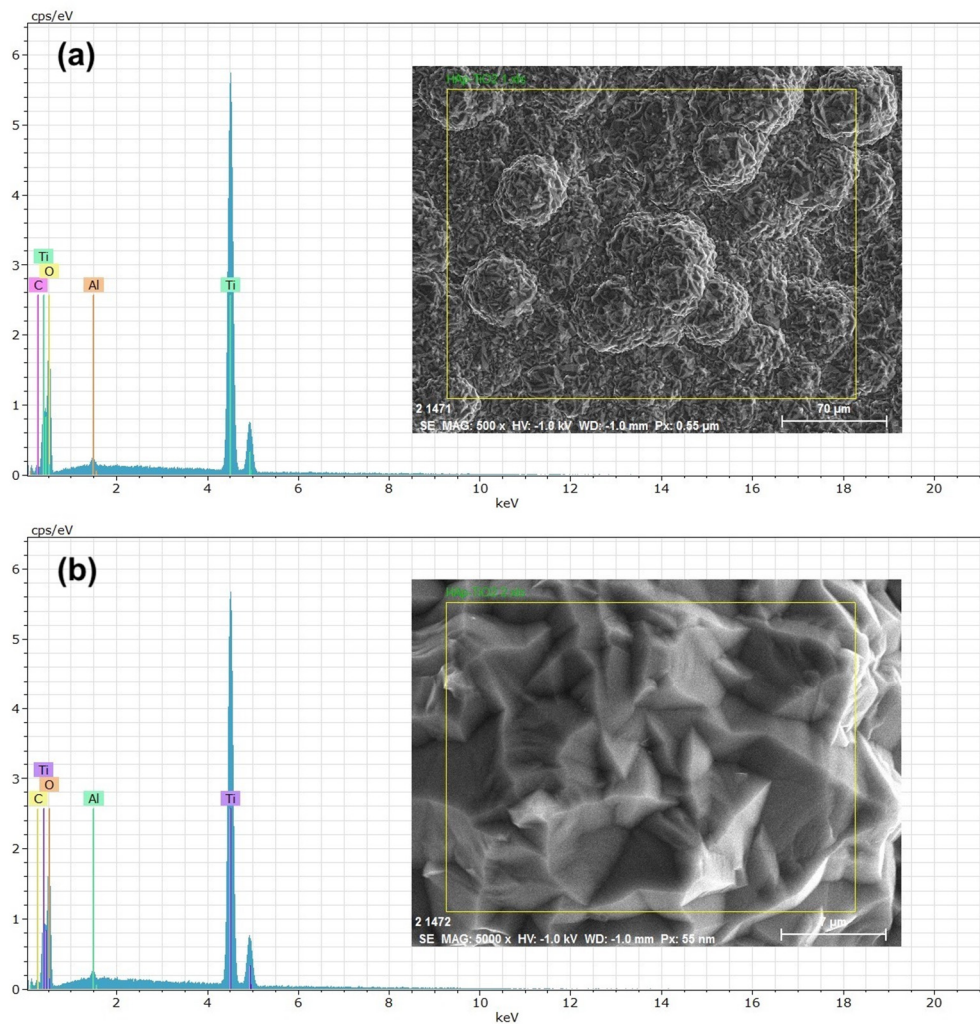


Figure 4. EDS spectra of TiO_2 coating: a) Micrograph at x500; b) micrograph at x5000.

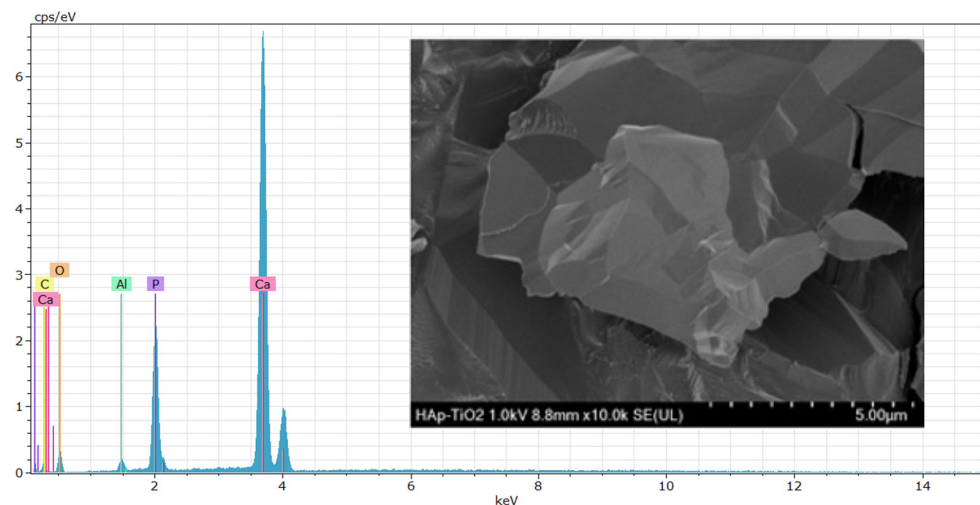


Figure 5. EDS spectra of HAp flakes.

4. Conclusions

We achieved the successful synthesis of hydroxyapatite flakes through the utilization of the microwave-assisted hydrothermal method. Notably, our investigation brought to light the significant impact of glutamic acid on the morphology of hydroxyapatite flakes, providing valuable insights into

their structure. Furthermore, we extended our study to include the synthesis of titanium dioxide (TiO_2) thin films utilizing hydroxyapatite flakes as a substrate. The X-ray diffraction (XRD) analysis revealed distinct diffraction peaks corresponding to the presence of hydroxyapatite on one side of the flake and TiO_2 in the anatase phase on the opposite side. This dual-phase formation is remarkable, showcasing the versatility of the hydroxyapatite substrate. Scanning electron microscopy (SEM) studies offer a detailed glimpse into the morphology of TiO_2 thin films, showcasing a homogeneous arrangement of faceted crystals with a prismatic appearance. The uniformity observed in this morphology enhances the potential applications of TiO_2 coating. Elemental analysis through energy-dispersive X-ray spectroscopy (EDS) has further supported our findings, elucidating the elemental composition of the coatings. This underscores the successful integration of hydroxyapatite flakes in TiO_2 thin films. Our study lays the groundwork for future investigations, suggesting that we should continue exploring the photocatalytic properties of the composite material obtained (HAp/TiO_2). Additionally, these compounds have a potential application in biomedicine as a biocompatible material in tissue regeneration.

The versatile coating technique employed, metal-organic chemical vapor deposition (MOCVD), emerges as a powerful tool, providing control over the thickness and structure of TiO_2 thin films.

Author Contributions: Conceptualization Néstor Méndez-Lozano; methodology Néstor Méndez-Lozano; software, investigation, Néstor Méndez-Lozano; writing—original draft preparation, Néstor Méndez-Lozano.; writing—review and editing, Eduardo E. Pérez-Ramírez.; supervision, Miguel de la Luz-Asunción; project administration, Eduardo E. Pérez-Ramírez.

Funding: This research received no external funding

Institutional Review Board Statement: Not applicable.

Informed Consent Statement: Not applicable.

Data Availability Statement: Data available on request from the authors.

Conflicts of Interest: The authors declare no conflict of interest.

References

1. Yu, J., & Zhao, X. Effect of substrates on the photocatalytic activity of nanometer TiO_2 thin films. *Materials Research Bulletin* **2000**, 35(8), 1293-1301. [https://doi.org/10.1016/S0025-5408\(00\)00327-5](https://doi.org/10.1016/S0025-5408(00)00327-5)
2. Franz, S., Falletta, E., Arab, H., Murgolo, S., Bestetti, M., & Mascolo, G. Degradation of carbamazepine by photo (electro) catalysis on nanostructured TiO_2 meshes: Transformation products and reaction pathways. *Catalysts* **2020**, 10(2), 169. <https://doi.org/10.3390/catal10020169>
3. Han, Z., Chang, V. W., Zhang, L., Tse, M. S., Tan, O. K., & Hildemann, L. M. Preparation of TiO_2 -coated polyester fiber filter by spray-coating and its photocatalytic degradation of gaseous formaldehyde. *Aerosol and Air Quality Research* **2012**, 12(6), 1327-1335. <https://doi.org/10.4209/aaqr.2012.05.0114>
4. Cotolan, N., Rak, M., Bele, M., Cör, A., Muresan, L. M., & Milošev, I. Sol-gel synthesis, characterization, and properties of TiO_2 and Ag-TiO_2 coatings on titanium substrate. *Surface and Coatings Technology* **2016**, 307, 790-799. <https://doi.org/10.1016/j.surfcoat.2016.09.082>
5. Lee, H., Song, M. Y., Jurng, J., & Park, Y. K. The synthesis and coating process of TiO_2 nanoparticles using CVD process. *Powder technology* **2011**, 214 (1), 64-68. <https://doi.org/10.1016/j.powtec.2011.07.036>
6. Komaraiah, D., Radha, E., Sivakumar, J., Reddy, M. R., & Sayanna, R. Photoluminescence and photocatalytic activity of spin coated Ag^+ doped anatase TiO_2 thin films. *Optical Materials* **2020**, 108, 110401. <https://doi.org/10.1016/j.optmat.2020.110401>
7. Dundar, I., Krichevskaya, M., Katerski, A., & Acik, I. O. TiO_2 thin films by ultrasonic spray pyrolysis as photocatalytic material for air purification. *Royal Society open science* **2019**, 6(2), 181578. <https://doi.org/10.1098/rsos.181578>
8. Latif, N. T., & Rzaij, J. M. Concentration Effect of Mixed SnO_2 - ZnO on TiO_2 Optical Properties Thin Films prepared by Chemical Spray Pyrolysis Technique. *J. Univ. Anbar pure Sci* **2020**, 14(1), 43-49. <http://dx.doi.org/10.37652/JUAPS.2020.14.1.8>

9. Sheng, G., Qiao, L., & Mou, Y. Preparation of TiO₂/hydroxyapatite composite and its photocatalytic degradation of methyl orange. *Journal of Environmental Engineering* **2011**, *137*(7), 611-616. [https://doi.org/10.1061/\(ASCE\)EE.1943-7870.0000357](https://doi.org/10.1061/(ASCE)EE.1943-7870.0000357).
10. Sánchez-Hernández, A. K., Martínez-Juárez, J., Gervacio-Arciniega, J. J., Silva-González, R., & Robles-Águila, M. J. Effect of ultrasound irradiation on the synthesis of hydroxyapatite/titanium oxide nanocomposites. *Crystals* **2020**, *10*(11), 959. <https://doi.org/10.3390/crust10110959>.
11. Méndez-Lozano, N., Velázquez-Castillo, R., Rivera-Muñoz, E. M., Bucio-Galindo, L., Mondragón-Galicia, G., Manzano-Ramírez, A., ... & Apátiga-Castro, L. M. Crystal growth and structural analysis of hydroxyapatite nanofibers synthesized by the hydrothermal microwave-assisted method. *Ceramics International* **2017**, *43*(1), 451-457. <https://doi.org/10.1016/j.ceramint.2016.09.179>
12. Apátiga, L. M., & Castaño, V. M. Magnetic behavior of cobalt oxide films prepared by pulsed liquid injection chemical vapor deposition from a metal-organic precursor. *Thin Solid Films* **2006**, *496*(2), 576-579. <https://doi.org/10.1016/j.tsf.2005.08.344>.
13. Mendez-Lozano, N., Apatiga-Castro, M., Soto, K. M., Manzano-Ramírez, A., Zamora-Antunano, M., & Gonzalez-Gutierrez, C. Effect of temperature on crystallite size of hydroxyapatite powders obtained by wet precipitation process. *Journal of Saudi Chemical Society* **2022**, *26*(4), 101513. <https://doi.org/10.1016/j.jscs.2022.101513>
14. Apátiga, L. M., Rubio, E., Rivera, E., & Castaño, V. M. Surface morphology of nanostructured anatase thin films prepared by pulsed liquid injection MOCVD. *Surface and Coatings Technology* **2006**, *201*(7), 4136-4138. <https://doi.org/10.1016/j.surfcoat.2006.08.016>
15. Burdusel, A. C., Neacsu, I. A., Birca, A. C., Chircov, C., Grumezescu, A. M., Holban, A. M., ... & Andronescu, E. Microwave-Assisted Hydrothermal Treatment of Multifunctional Substituted Hydroxyapatite with Prospective Applications in Bone Regeneration. *Journal of Functional Biomaterials* **2023**, *14*(7), 378. <https://doi.org/10.3390/jfb14070378>
16. Galenda, A., Natile, M. M., & El Habra, N. Large-Scale MOCVD Deposition of Nanostructured TiO₂ on Stainless Steel Woven: A Systematic Investigation of Photoactivity as a Function of Film Thickness. *Nanomaterials* **2022**, *12*(6), 992. <https://doi.org/10.3390/nano12060992>
17. Cotrut, C. M., Vladescu, A., Dinu, M., & Vraneanu, D. M. Influence of deposition temperature on the properties of hydroxyapatite obtained by electrochemical assisted deposition. *Ceramics International* **2018**, *44*(1), 669-677. <https://doi.org/10.1016/j.ceramint.2017.09.227>
18. Miculescu, F., Luță, C., Constantinescu, A. E., Maidaniuc, A., Mocanu, A. C., Miculescu, M., ... & Ciocan, L. T. Considerations and influencing parameters in EDS microanalysis of biogenic hydroxyapatite. *Journal of Functional Biomaterials* **2020**, *11*(4), 82. <https://doi.org/10.3390/jfb11040082>

Disclaimer/Publisher's Note: The statements, opinions and data contained in all publications are solely those of the individual author(s) and contributor(s) and not of MDPI and/or the editor(s). MDPI and/or the editor(s) disclaim responsibility for any injury to people or property resulting from any ideas, methods, instructions or products referred to in the content.